

Journal Pre-proof

Activation of Siglec-7 results in inhibition of in vitro and in vivo growth of human mast cell leukemia cells

Nadine Landolina, Ilan Zaffran, Dubravka Smiljkovic, Eva Serrano-Candelas, Dominik Schmiedel, Sheli Friedman, Michel Arock, Karin Hartmann, Eli Pikarsky, Ofer Mandelboim, Margarita Martin, Peter Valent, Francesca Levi-Schaffer



PII: S1043-6618(19)32563-0
DOI: <https://doi.org/10.1016/j.phrs.2020.104682>
Reference: YPHRS 104682

To appear in: *Pharmacological Research*

Received Date: 12 November 2019
Revised Date: 31 January 2020
Accepted Date: 4 February 2020

Please cite this article as: Landolina N, Zaffran I, Smiljkovic D, Serrano-Candelas E, Schmiedel D, Friedman S, Arock M, Hartmann K, Pikarsky E, Mandelboim O, Martin M, Valent P, Levi-Schaffer F, Activation of Siglec-7 results in inhibition of in vitro and in vivo growth of human mast cell leukemia cells, *Pharmacological Research* (2020), doi: <https://doi.org/10.1016/j.phrs.2020.104682>

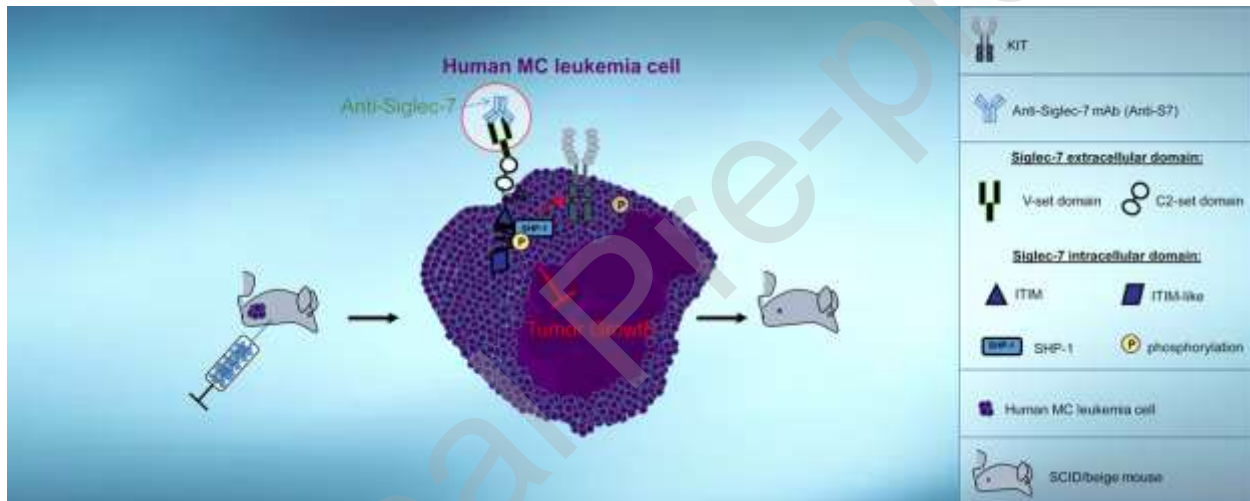
This is a PDF file of an article that has undergone enhancements after acceptance, such as the addition of a cover page and metadata, and formatting for readability, but it is not yet the definitive version of record. This version will undergo additional copyediting, typesetting and review before it is published in its final form, but we are providing this version to give early visibility of the article. Please note that, during the production process, errors may be discovered which could affect the content, and all legal disclaimers that apply to the journal pertain.

© 2020 Published by Elsevier.

Activation of Siglec-7 results in inhibition of in vitro and in vivo growth of human mast cell leukemia cells

Nadine Landolina^{1*}, Ilan Zaffran^{1*}, Dubravka Smiljkovic², Eva Serrano-Candelas^{3,4}, Dominik Schmiedel⁵, Sheli Friedman¹, Michel Arock⁶, Karin Hartmann⁷, Eli Pikarsky⁵, Ofer Mandelboim⁵, Margarita Martin^{3,4}, Peter Valent^{2,8}, Francesca Levi-Schaffer^{1**}

Graphical abstract



Affiliations:

¹Pharmacology & Experimental Therapeutics Unit, Institute for Drug Research, School of Pharmacy, Faculty of Medicine, The Hebrew University of Jerusalem, Israel;

²Department of Internal Medicine I, Division of Hematology and Hemostaseology, Medical University of Vienna, Vienna, Austria;

³Biochemistry Unit, Biomedicine Department, Faculty of Medicine, University of Barcelona, Barcelona, Spain;

⁴Laboratory of Clinical and Experimental Respiratory Immunoallergy, IDIBAPS, Barcelona, Spain,

⁵The Lautenberg Center for General and Tumor Immunology, The Hebrew University Hadassah Medical School, IMRIC, Jerusalem, Israel;

⁶Biological Haematology Department, Pitié-Salpêtrière Hospital, Paris;

⁷Department of Dermatology, University of Luebeck, Luebeck, Germany;

⁸Ludwig Boltzmann Institute for Hematology and Oncology, Medical University of Vienna, Austria.

*These authors contributed equally: Nadine Landolina, Ilan Zaffran

Running title: Siglec-7 activation inhibits mast cell leukemia cell growth

****Correspondence:** Prof. Francesca Levi-Schaffer, Isaac & Myrna Kaye Chair in Immunopharmacology, Pharmacology & Experimental Therapeutics Unit, Institute for Drug Research, School of Pharmacy, Faculty of Medicine, The Hebrew University of Jerusalem Jerusalem, Israel, Tel: +972-2-6757512; Fax: 972-2-6758144 E-mail: francescal@ekmd.huji.ac.il

Abstract

Advanced systemic mastocytosis is a rare and still untreatable disease. Blocking antibodies against inhibitory receptors, also known as "immune checkpoints", have revolutionized anti-cancer treatment. Inhibitory receptors are expressed not only on normal immune cells, including mast

cells but also on neoplastic cells. Whether activation of inhibitory receptors through monoclonal antibodies can lead to tumor growth inhibition remains mostly unknown. Here we show that the inhibitory receptor Siglec-7 is expressed by primary neoplastic mast cells in patients with systemic mastocytosis and by mast cell leukemia cell lines. Activation of Siglec-7 by anti-Siglec-7 monoclonal antibody caused phosphorylation of Src homology region 2 domain-containing phosphatase-1 (SHP-1), reduced phosphorylation of KIT and induced growth inhibition in mast cell lines. In SCID-beige mice injected with either the human mast cell line HMC-1.1 and HMC-1.2 or with Siglec-7 transduced B cell lymphoma cells, anti-Siglec-7 monoclonal antibody reduced tumor growth by a mechanism involving Siglec-7 cytoplasmic domains in “preventive” and “treatment” settings. These data demonstrate that activation of Siglec-7 on mast cell lines can inhibit their growth *in vitro* and *in vivo*. This might pave the way to additional treatment strategies for mastocytosis.

Keywords: Mastocytosis, activation, inhibitory receptor, monoclonal antibody, SHP-1, ITIM.

Abbreviations

Anti-Siglec-7 mAb (Anti-S7), Bone Marrow (BM), human mast cell leukemia comprising both HMC-1.1. and HMC-1.2 (HMC-1), indolent systemic mastocytosis (ISM), inhibitory receptor (IR), intraperitoneal (ip), Immunoreceptor Tyrosine based Inhibitory Motif (ITIM), mast cells (MCs), mast cell leukemia (MCL), monoclonal antibody (mAb), natural killer cells (NK), Src homology 2–containing inositol polyphosphate 5-phosphatase (SHIP), Src homology region 2 domain-containing phosphatase-1 (SHP-1), sialic acid binding Ig-like lectin-7 (Siglec-7), subcutaneous (sc), systemic mastocytosis (SM), systemic mastocytosis with an associated hematologic neoplasm (SM-AHN), aggressive SM (ASM), SM with an associated hematologic neoplasm (SM-AHN), ASM with associated acute myeloid leukemia (ASM-AML).

1. Introduction

Inhibitory receptors (IRs) are surface receptors that signal primarily after phosphorylation of their cytoplasmic immunoreceptor tyrosine-based inhibitory motifs (ITIMs) domains and consequent recruitment of the Src homology 2–containing inositol polyphosphate 5-phosphatase (SHIP), Src homology region 2 domain-containing phosphatase-1 (SHP-1) or SHP-2 (reviewed in Billadeauf(1)). SHP-1 signal transduction pathways lead to modulation of various cellular activities including downregulation of immune cell activation(2, 3), induction of cytotoxicity(4), cell cycle arrest(5) and apoptosis(6).

Siglec-7 is an IR belonging to the type-I immunoglobulin superfamily-lectins(7) expressed on human but not murine immune cells(8, 9), including mast cells (MCs)(10) and eosinophils(11). Once Siglec-7 is activated by its natural ligands (preferably α 2, 6-linked disialic gangliosides and α 2, 8-linked gangliosides) or through specific monoclonal antibodies (mAbs), it inhibits natural killer cell (NK) cytotoxicity (12), IgE-dependent MC activation(10) and granulocyte-macrophage colony-stimulating factor -induced eosinophil activation(13).

Siglec-7 is also expressed on neoplastic cells. For example, Siglec-7 expression has been previously reported on acute myeloid leukemia cells (AML) belonging to M4 and M5 subtypes (14) and its engagement by mAbs has been shown to slightly inhibit *in vitro* proliferation of chronic myeloid leukemia cells (CML) *via* undefined mechanisms (15).

Mastocytosis is a rare disease characterized by aberrant growth and accumulation of clonal MCs in several different organ systems, including the bone marrow (BM).(16-18) According to the World Health Organization classification, mastocytosis is divided into cutaneous mastocytosis, indolent systemic mastocytosis (ISM), smoldering SM, SM with an associated hematologic

neoplasm (SM-AHN), aggressive SM (ASM), mast cell leukemia (MCL) and MC sarcoma (17, 19, 20).

In most patients with mastocytosis, neoplastic cells display gain-of-function mutations of the type III tyrosine kinase (TK) receptor KIT (21-23) resulting in enhanced survival and autonomous growth of MCs (24, 25). The most common *KIT* mutation found in SM patients is D816V (21, 23, 26). Downstream signaling pathways involve several key molecules such as signal transducer and activator of transcription 5 (STAT5) (27), phosphoinositide 3-kinase (PI3K)/protein kinase B(AKT) (28) and the mechanistic target of rapamycin (mTOR) (29). Several human MCL cell lines have been established in the past. The cell lines commonly employed in mastocytosis research are HMC-1.1 possessing the G560V *KIT* mutation, but not the D816V mutation, the HMC-1.2 cell line possessing both, the G560V *KIT* and the D816V *KIT* mutations (30), the LAD2 cell line (31), and the ROSA^{KIT^{D816V}} cell line (32).

Whereas patients with ISM have an excellent prognosis and therefore do not require intensive therapies, patients with advanced SM (ASM, SM-AHN, MCL) have a poor prognosis with short survival times (16-18). Therefore, these patients are candidates for interventional anti-neoplastic therapies. In young and fit patients with ASM and MCL, polychemotherapy and hematopoietic stem cell transplantation can be offered. However, in older co-morbid patients less intensive chemotherapy like cladribine, targeted drugs such as Midostaurin or interferon-alpha are usually prescribed.(16-18, 33, 34). Although these drugs are quite effective, many of the patients relapse after some time or have an upfront resistant disease. For these patients, alternative drugs and new experimental agents have to be considered (35, 36).

In this study, we investigated the expression of Siglec-7 on MCs in mastocytosis patients and asked whether activation of Siglec-7 on MCL cell lines might inhibit their growth *in vitro* and *in vivo*.

2. Materials and Methods

2.1 Patient samples

BM cells were obtained from patients with ISM (n=5), ASM (n=2), SM-AHN (n=2) or MCL (n=1) during routine investigations. The two patients with SM-AHN were suffering from ASM with an associated myelodysplastic/myeloproliferative overlap neoplasm (ASM-MDS/MPN; n=1) and ASM with associated acute myeloid leukemia (ASM-AML; n=1). BM cells were stored frozen in liquid nitrogen in a biobank before used. Control BM samples were obtained from two patients with multiple myeloma (MM) and one with a Non-Hodgkin lymphoma (NHL). The patients' characteristics are shown in Table 1.

2.2 Cells and cell cultures

HMC-1.1 and HMC-1.2 cell lines(37) were kindly provided by Dr. Joseph H. Butterfield (Mayo Clinic, Rochester, MN, USA) and cultured in Iscove's modified Dulbecco's medium (IMDM, Gibco-ThermoFisher, Waltham, MA, USA) supplemented with 10% fetal bovine serum (FBS, Sigma, St. Louis, MO, USA), penicillin (100 IU/ml), streptomycin (100 µg/ml) (Biological Industries, Beit Haemek, Israel), and α -Thioglycerol (1.2 mM, Sigma). Both HMC-1 cell lines were passaged every 3-4 days. LAD2 cells(31) were kindly provided by Drs. A. Kirshenbaum and D. Metcalfe (NIH, Bethesda, MD, USA) and were grown in Stem-Pro medium containing Stem-Pro supplement (Gibco-ThermoFisher), L-glutamine (2 mM), penicillin (100 IU/ml), streptomycin (100 µg/ml) (Biological Industries) and human stem cell factor (SCF,100 ng/ml, a generous gift from Swedish Orphan Biovitrum (Sobi) (Stockholm, Sweden). Half of the cell culture medium was replaced weekly with fresh culture medium.

ROSA^{KIT WT} and ROSA^{KIT D816V} cells were cultured in IMDM in the presence of SCF-containing supernatants (10%) of Chinese hamster ovary cells transfected with murine *scf* and 10% heat-inactivated FCS. The human lymphoblastoid B cell line RPMI-8866 (ATCC, Rockville, MD, USA) and transfectants were cultured in RPMI-1640 (Gibco-ThermoFisher) supplemented with 10% FBS, L-glutamine (2 mM), penicillin (100 IU/ml) + streptomycin (100 µg/ml) (Biological Industries). RPMI-8866 transfectants were generated using lentiviral transduction and sorted according to their GFP reporter expression to obtain uniform expression, like outlined in the supplemental methods section. All cell lines were cultured at 37°C in 5% CO₂ and periodically checked for Siglec-7 membrane expression by flow cytometry (FC).

2.3 Cell viability

HMC-1.1 cells ($7 \times 10^3/100\mu\text{l}$) or LAD2 cells ($20 \times 10^3/100\mu\text{l}$) in their respective culture medium, were seeded in flat bottom 96 well cell culture plates (Thermo Scientific Nunc, Israel) with Anti-Siglec-7 mAb (clone QA79, 10µg/ml, azide-free) or with an isotype-matched control IgG1 (mouse IgG1 K Isotype Control Purified, 10 µg/ml, azide-free) both purchased from eBioscience (ThermoFisher). The concentration of 10 µg/ml for Anti-Siglec-7 was found to be optimal following a dose-response calibration curve. The mAbs were added on the first day of the experiment and no additional medium or mAbs were added during the culture time up to 4 days. Trypan blue (Sigma) exclusion test was used to determine numbers of viable cells at 24, 48, 72 and 96 hours (h) of culture.

Cell viability of HMC-1.1, HMC-1.2 cells ($1 \times 10^4/100\mu\text{l}$), LAD2 cells ($3 \times 10^4/100\mu\text{l}$) and Siglec-7 transduced RPMI 8866 cell lines ($3 \times 10^3/100\mu\text{l}$, see below) was also determined by MTT assay (Sigma), according to manufacturer's instructions, after culturing the cells with Anti-Siglec-7 mAb (10µg/ml) or control IgG1 (10 µg/ml) or medium alone for 72 h.

2.4 FC

Analysis of Siglec-7 surface expression on primary mast cells (MC) and MCs lines (ROSA^{KIT WT} cells and ROSA^{KIT 816V}) was performed after incubation with Fc-blocking reagent and staining with monoclonal antibodies (mAb) including PE-labeled anti-Siglec-7 mAb clone QA79 (eBiosciences) or clone 6-434 (Biolegend). Bone marrow (BM) MC were obtained from SM patients (ISM, ASM, SM-AHN and MCL) or patients with lymphoproliferative neoplasms. Expression of Siglec-7 was analyzed by FC on a FACS Canto (BD Biosciences). A detailed description of FC is provided in the Supplement.

2.5 Generation of Siglec-7 and RPMI-8866 mutant subclones by transfection

The inserts for the expression vectors encoding full-length Siglec-7, or mutants lacking both ITIM-like and ITIM generated by PCR, cloning and transfection procedures in 8866 cells are described in the Supplement.

2.6 Mouse mastocytosis xenograft model

SCID-beige mice (males, 6-7 weeks old, Harlan, ENVIGO, UK) were maintained in SPF conditions. Mice were shaved in the flank and injected subcutaneously (sc) with HMC-1.1 or HMC-1.2 or with Siglec-7 transduced RPMI 8866 cell lines (0.5×10^6 /100 μ l ice cold PBS).

In the “preventive” protocol, mice (6-7/group) were injected intraperitoneally (i.p) with either anti-Siglec-7 or IgG1 (4 μ g/kg in 100 μ l ice cold PBS), 30 minutes (min) after either HMC-1.1, HMC-1.2 or Siglec-7 transduced RPMI 8866 tumor cell inoculation and every other day until tumors reached ~1.5 cm by caliper measurement (according to Hebrew University ethical animal guidelines). Mice were consequently euthanized (Figure 4A). In the "treatment" protocol, mice (10/ group) were injected ip with either Anti-Siglec-7 or IgG1 (8 μ g/ kg in 100 μ l ice cold PBS) from the day on which the tumor was visible and palpable (day 20 from inoculation) and then

every other day until tumors reached ~1.5 cm. At that time, mice were euthanized (Figure4D). Mice of all the experiments were checked every other day for tumor growth using the caliper and for changes in weight or signs of sickness. Upon euthanasia, tumors were excised, weighted and divided into different sections for further immunohistochemical (4% paraformaldehyde) and Western Blot analyses.

2.7 Histochemistry & Immunohistochemistry

Histochemistry and immunohistochemistry were performed on paraffin-embedded tissue samples as described in the Supplement.

2.8 Western Blot

Western Blot analysis was performed according to standard procedures on lysates from HMC-1.1 cells and from excised tumors (13). Membranes were probed with the following antibodies: anti-phospho-SHP-1 and anti-SHP-1 (each 1:200, Santa Cruz Technology, Santa Cruz, CA, USA), anti-phospho-Bcl2 (Ser 70), Bcl2, anti-phospho-KIT and anti-KIT (each 1:1000, Cell Signaling Technology), anti-Vinculin and anti-GAPDH (1:1000, Santa Cruz Technology). Signal was acquired using BioRad Chemi Doc XRS + Gel imaging system and bands quantified using Image Lab software.

2.9 Statistical analysis

Data are expressed as the mean \pm standard deviation (SD). Unpaired two-tailed Student's t-test (Excel) was used to examine statistical significance. $P < 0.05$ was considered statistically significant.

3. Results

3.1 Siglec-7 is expressed on MCs obtained from mastocytosis patients and on ROSA cell lines

In this study, by FC analysis, we have established that CD34⁻/CD45⁺/CD117⁺ BM MCs (dead cell exclusion test was not used; for gating strategy see Supplementary Figure 1)) obtained from patients with ISM (n=5), ASM (n=2), SM-AHN (n=2), or MCL (n=1) all stained positive for surface Siglec-7 with two different mAbs (QA and 6434), independently of the variant of SM (shown as dot plots in Figure 1 and histograms in Supplementary Figure 2 and Table 1). Interestingly, Siglec-7 was also found to be expressed on MCs in BM samples obtained from patients with lymphoproliferative neoplasms, without major differences in staining intensities when comparing MCs in control BM and BM MCs of mastocytosis patients (Supplementary Figure 3). Moreover, we have found that both ROSA^{KIT^{WT}} cells and ROSA^{KIT^{816V}} cell lines express Siglec-7 (Supplementary Figure 4) as previously shown for normal human MCs and the MCL cell lines HMC-1.1, HMC-1.2 and LAD2 (10).

New Figure 1:

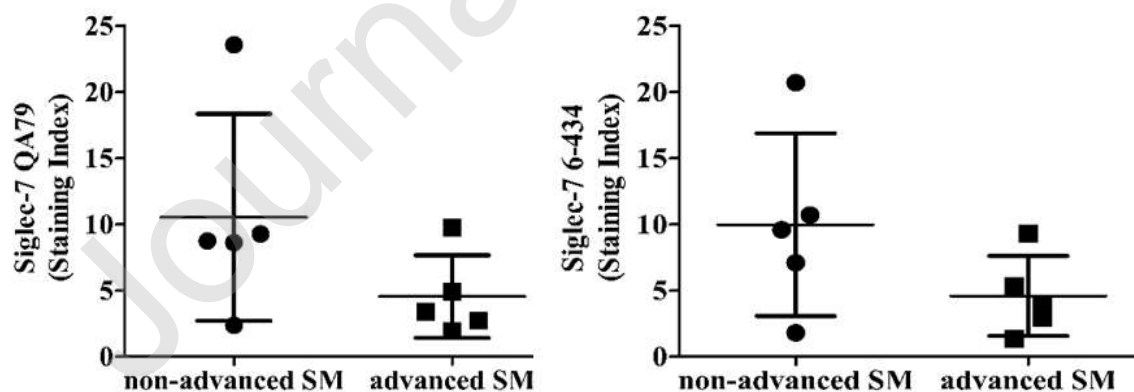


Figure 1- Siglec-7 is expressed on neoplastic mast cells (MCs) in systemic mastocytosis.

Bone marrow (BM) cells were obtained from patients with indolent systemic mastocytosis (ISM, n=5) or advanced SM, including aggressive SM (ASM; n=2), SM with an associated hematologic neoplasm (AHN, n=2) or MC leukemia (MCL, n=1). Patients with AHN were suffering from ASM with an associated myelodysplastic/myeloproliferative overlap neoplasm (ASM-MDS/MPN; n=1) or from ASM with associate acute myeloid leukemia (ASM-AML; n=1). BM cells were stained with two monoclonal antibodies against Siglec-7, QA79 (left plot) or 6-434 (right plot) by multicolor FC as described in the text. Surface expression of Siglec-7 on CD34⁻/CD45⁺/CD117⁺ MC was determined as median fluorescence intensity (MFI) and expressed as staining-index (SI) according to the formula: $SI = MFI (\text{test mAb}) / MFI (\text{isotype-control mAb})$.

Table 1:

Patient #	Diagnosis	Gender	Age (years)	WBC, G/L	Hb, g/dL	Serum tryptase $\mu\text{g/L}$	KIT D816V mutation	% of MC infiltration in BM	Siglec-7 (QA79)		Siglec-7 (6-434)	
									Staining Index Score		Staining Index Score	
1	ISM	M	45	5.81	17.6	35.4	-	5	2.38	±	1.80	±
2	ISM	M	53	6.58	12.7	40.9	+	40	8.62	+	9.58	+
3	ISM	F	27	6.50	13.0	36.7	+	10	9.28	+	10.70	++
4	ISM	F	47	9.39	14.6	34.9	+	5-10	23.57	++	20.70	++
5	ISM	M	68	9.03	12.6	83.3	+	10	8.75	+	7.10	+
6	ASM-MDS/MPN	M	78	27.50	8.2	45.9	+	10	1.94	±	1.37	±
7	ASM	M	63	33.50	10.9	80	+	20-25	2.73	±	4.03	+
8	ASM	M	71	21.55	8.3	97.1	+	5-10	4.90	+	5.33	+
9	ASM-AML	M	65	4.62	9.0	37.8	-	25	9.77	+	9.32	+
10	MCL	M	91	3.32	8.6	49.6	+	10	3.38	±	2.90	±
11	MM	M	49	5.00	13.4	N/A	N/A	N/A	7.25	+	2.64	±
12	MM	M	77	7.29	9.9	N/A	N/A	N/A	1.31	±	2.11	±
13	NHL	M	50	17.57	11.5	N/A	N/A	N/A	1.98	±	5.97	+

Old table 1:

Table 1- Patients' characteristics and expression levels of Siglec-7 on primary neoplastic mast cells (MCs) and MCs in control bone marrow (BM) samples.

Staining index (SI) for Siglec-7 (clones: QA79 and 6-434) obtained with MCs from patients with non-advanced and advanced SM and in control BM samples. Bone marrow (BM) cells were obtained from patients with indolent systemic mastocytosis (ISM, n=5) or advanced SM, including aggressive SM (ASM; n=2), SM with an associated hematologic neoplasm (AHN, n=2) or MC leukemia (MCL, n=1). Patients with AHN were suffering from ASM with an associated myelodysplastic/myeloproliferative overlap neoplasm (ASM-MDS/MPN; n=1) or from ASM with associate acute myeloid leukemia (ASM-AML; n=1). Expression of Siglec-7 on BM MCs was determined by multi-color flow cytometry (FC) using isotype-matched control antibodies and two monoclonal antibodies (mAb) against Siglec-7, namely QA79 and 6-434 as described in the text.

Surface expression of Siglec-7 on CD34-/CD45+/CD117+ MCs was determined as median fluorescence intensity (MFI) and expressed as staining-index (SI) according to the formula: $SI = MFI(\text{test mAb}) / MFI(\text{isotype-control Ab})$. Results were scored as follows: SI 0-1.3, -; SI 1.31-3, ±; SI 3.01-10, +; SI >10, ++. *BM infiltration with neoplastic MCs was determined by immunohistochemistry using an antibody against tryptase. WHO, World Health Organization.

3.2 Siglec-7 activation on MCL cell lines down-regulates their viability

In the present work, we asked whether Siglec-7 activation by specific mAbs will inhibit transformed MCs growth. To test this hypothesis, we incubated HMC-1.1, HMC-1.2 and LAD2 cells with Anti-Siglec-7 mAb or the isotype control (IgG1). Anti-Siglec-7 (10µg/ml, optimal concentration), significantly decreased the viability (MTT assay) of all the 3 cell lines at 72 h of culture to $66 \pm 11\%$, $71 \pm 6\%$ and $87 \pm 3\%$ viable cells (mean \pm SD, *** $p < .0005$), (Figure 2A), for HMC-1.1, HMC-1.2 and LAD2 respectively). Moreover, the numbers of viable HMC-1.1 (Figure 2B) and LAD2 cells (Supplementary Figure 5A) as determined by Trypan Blue staining, were significantly reduced in cultures containing Anti-Siglec-7 in a time-dependent fashion. At 24, 48 and 72 h, viable HMC-1.1 in Anti-Siglec-7 treated cultures were respectively 7036 ± 1373 , 10150 ± 1616 and 15500 ± 2166 cells/ml, mean \pm SD, and in IgG1 treated cultures were respectively 10281 ± 1218 cells/ml ($p^{***} < .0005$), 13869 ± 2192 (* $p < .05$) and 25226 ± 3190 mean \pm SD (*** $p < .0005$) (Figure 2B). In LAD2, the decrease in viable cells in Anti-Siglec-7 cultures was significantly different from the ones in IgG1 only at 72h (33260 ± 2789 vs 42625 ± 2473 cells/ml, * $p = 0.0458$) (Supplementary Figure 5A).

Therefore, it seems that Anti-Siglec-7 mediated inhibition of survival is more pronounced in HMC-1 cells than in LAD2 cells. Nevertheless, no signs of apoptosis as assessed by cleaved Caspase3 and Annexin V staining could be detected in HMC-1.1 after *in vitro* exposure to Anti-

Siglec-7 mAb (not shown). Cell numbers in Anti-Siglec-7 treated HMC-1.1 and LAD2 were significantly reduced, as expected, also following Midostaurin (1 μ M) incubation at all three time points assessed. Importantly, cell surface expression of Siglec-7 was stable on HMC-1.1 and LAD2 cells even after a 72h treatment with Anti-Siglec-7 (Figure 2C and Supplementary Figure 5B).

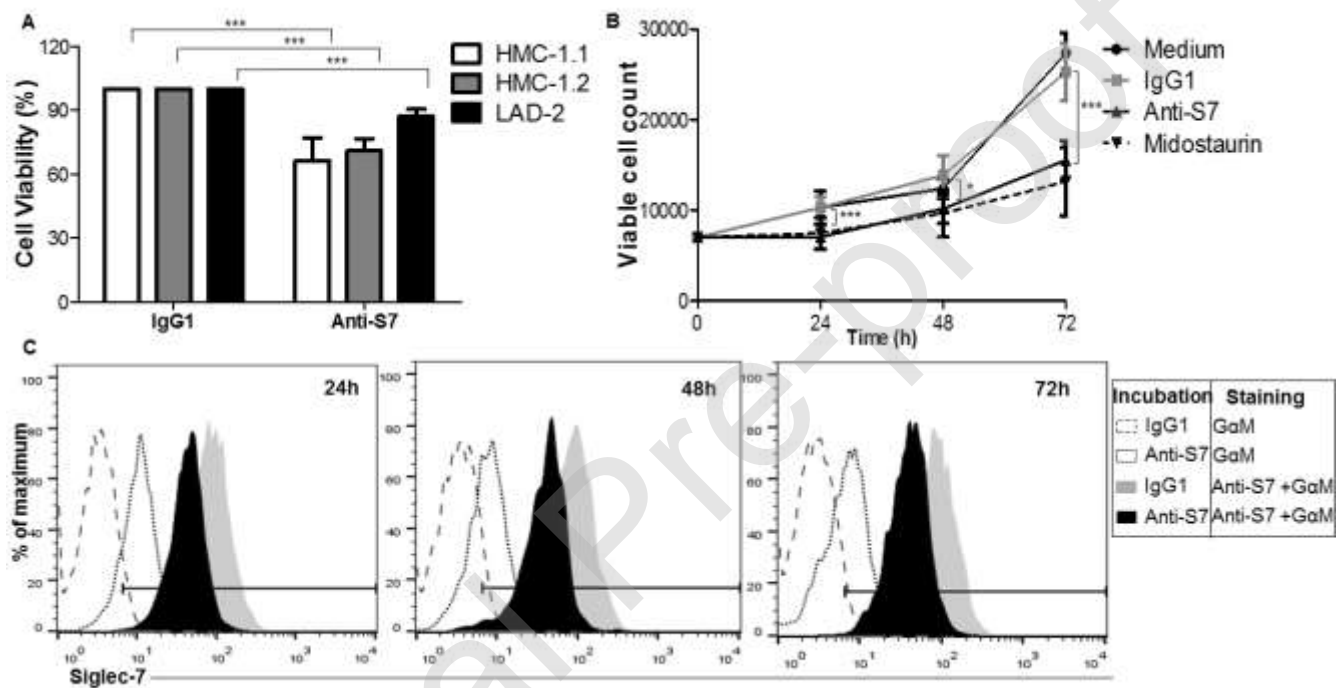


Figure 2- Siglec-7 activation down-regulates survival of mast cell leukemia (MCL) cell lines.

(A) Cell viability of HMC-1.1, HMC-1.2 and LAD2 cells treated with Anti-Siglec-7 mAb (10 μ g/ml) or control IgG1 (10 μ g/ml) for 72 hours (h) by MTT assay. Data are expressed as mean \pm SD (%) of viable cells, calculated by dividing numbers of Anti-Siglec-7-treated cells by numbers of IgG1 treated cells multiplied by 100. n=3, Anti-Siglec-7 vs IgG1, ***: p<.0005.

(B) Numbers of Trypan blue negative HMC-1.1 cells (cells/ml) treated with Anti-Siglec-7 or IgG1 for different time points. Data are expressed as mean \pm SD. n=5. Anti-Siglec-7 vs IgG1, *, p<.05 at 48 h; ***, p<.0005 at 24 and 72 h. (C) FC analysis (% of maximum) of Siglec-7 expression on

HMC-1.1 cells after treatment (24, 48, or 72 h) with Anti-Siglec-7 mAb or IgG1. Afterwards cells were incubated with strip buffer in order to eliminate bound Ab and stained with Anti-Siglec-7 and goat anti-mouse Ab (647GaM Ab) or with 647GaM Ab alone. The histograms are representative of 3 independent experiments.

3.3 Siglec-7 activation on HMC-1.1 cells causes recruitment of SHP-1 and de-phosphorylation of KIT and its downstream signaling pathway molecules

Next, we tested whether SHP-1 is phosphorylated following activation of Siglec-7 on HMC-1.1 cells. As can be seen in Figure 3A, SHP-1 is phosphorylated as early as 2 min after incubation with Anti-Siglec-7 ($295.56\% \pm 123.06$, $*p=0.0409$). SHP-1 has been found to interact with KIT by binding selectively to the phosphorylated KIT juxtamembrane region and to negatively regulate KIT-mediated cell proliferation (39). We therefore hypothesized that Siglec-7 might exert its effects at least in part *via* de-phosphorylation of KIT and possibly also by inhibition of RAS/RAF and JAK/STAT signaling pathways. HMC-1.1 cells incubated with Anti-Siglec-7 displayed a reduction, even if not significant, in KIT phosphorylation after 30 min ($17.48\% \pm 13.25$, Western Blot) (Figure 3B) as well as in KIT downstream signaling molecules, i.e. SYK, STAT6, ERK and AKT (data not shown).

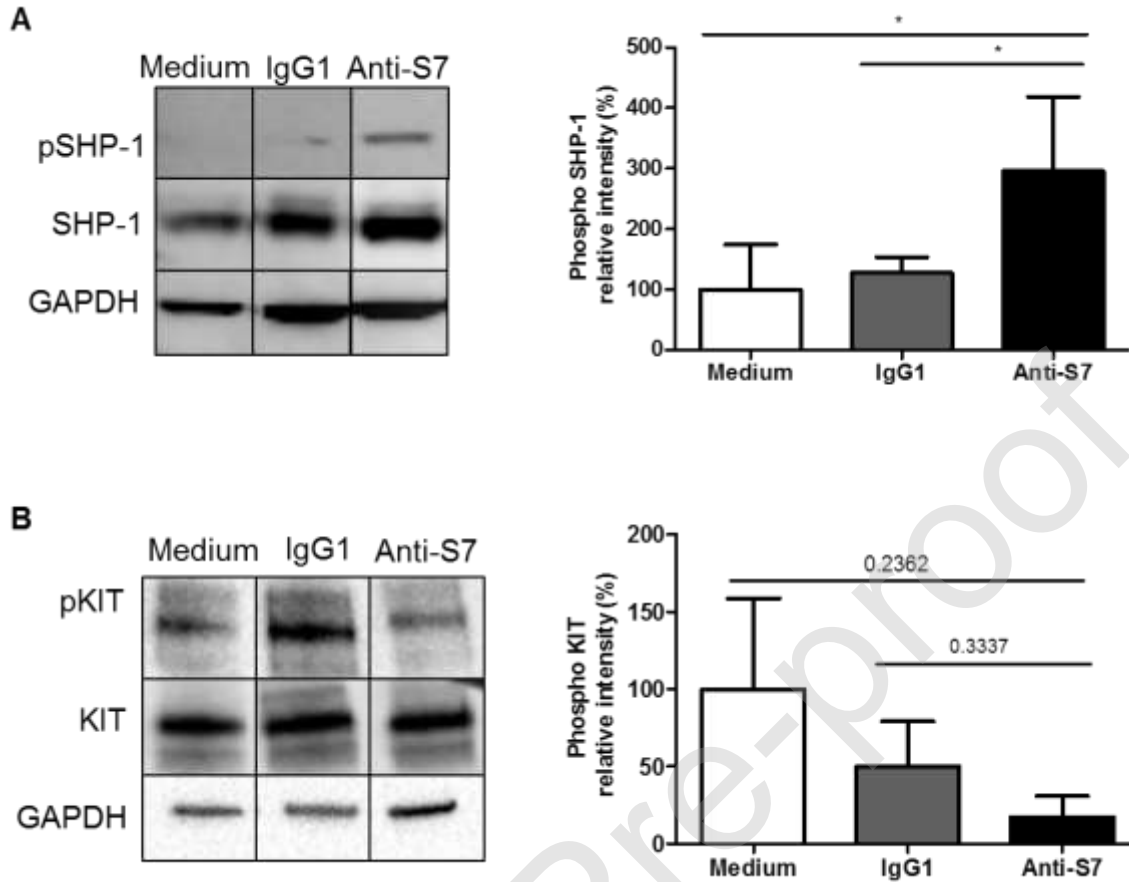


Figure 3- Siglec-7 activation on HMC-1.1 cells causes recruitment of SHP-1 and dephosphorylation of KIT.

HMC-1.1 cells were incubated in medium, or with Anti-Siglec-7 mAb or with IgG1 for different time periods as indicated. (A) Phosphorylation of SHP-1 at 2 min as assessed by Western Blot analysis using Abs against phosphorylated SHP-1 (pSHP-1) and total SHP-1 and GAPDH as a loading control and quantified by densitometry. The blot is a representative of 5 independent experiments. Western Blot densitometry values were obtained by dividing the intensity of each band by the loading control and then by the total SHP-1 protein. Data are expressed as mean \pm SD, % of phosphorylated SHP-1,

(B) Phosphorylation of KIT at 30 min as assessed by Western Blot analysis using Abs against phosphorylated KIT (pKIT) and total KIT and GAPDH as a loading control and quantified by densitometry. Western Blot densitometry graphs were obtained as described in A. The blot is a representative of 3 independent experiments.

3.4 Anti-Siglec-7 inhibits the development of HMC-1.1 tumor growth in SCID-beige mice by apoptosis and by cell cycle arrest

Finally, we aimed to test the effect of Anti-Siglec-7 *in vivo* in MCL xenograft models. For this, we injected HMC-1.1 or HMC-1.2 cells (0.5×10^6) sc into SCID-beige mice (40) followed by Anti-Siglec-7 or IgG1 ip treatment. We initially employed the “preventive” protocol in which mice were injected with Anti-Siglec-7 mAb or with an IgG1 (4 μ g/kg), 30 min after tumor cell injection (day 1) and thereafter, every other day until tumor size reached ~1.5 cm (Figure 4A). At this point (day 50), mice were euthanized, and tumors were excised. In both HMC-1.1 and HMC-1.2 bearing mice injected with Anti-Siglec-7, tumor weight was significantly reduced as compared with mice injected with the control Ab. In HMC-1.1 grafted mice, values for anti-Siglec-7 treated mice were 173 ± 55 mg, mean \pm SD and for IgG1 treated mice 398 ± 84 mean \pm SD (n=12 mice from 2 different pooled experiments *p< 0.05 Figure 4B). In HMC-1.2 grafted mice, values were 33260 ± 2789 mean \pm SD for anti-Siglec-7 treated mice and 42625 ± 2473 mean \pm SD for IgG1 treated mice (n=14 mice from 2 different pooled experiments, p*=0.0378 (Supplementary Figure 6).

Immunohistochemical staining of the Anti-Siglec-7 treated HMC-1.1 tumors with anti-cleaved Caspase-3 (Figure 4C upper panel), anti-phosphohistone-3 (Figure 4C middle panel) and anti-phospho-KIT (Supplementary Figure 7) revealed a significant increase in the number of apoptotic cells (for anti-Siglec-7 30 ± 17 and 14 ± 10 for IgG1 treated mice slides *p< 0.05 Figure 4C upper

panel), decrease in mitosis (6 ± 2 mean \pm SD for anti-Siglec-7 treated mice slides and 9 ± 4 mean \pm SD for IgG1 treated mice slides $*p < 0.05$ (Figure 4C middle panel) and KIT de-phosphorylation (0.008 ± 0.010 mean \pm SD for anti-Siglec-7 treated mice slides and 0.016 ± 0.017 mean \pm SD for IgG1 treated mice slides $***p < 0.0005$ (Supplementary Figure 7) indicating induction of apoptosis, and cell cycle inhibition *in vivo*. In line with these observations, MCs numbers, evaluated by Toluidine blue staining, were markedly reduced upon Anti-Siglec-7 treatment (49.56 ± 20.23 mean \pm SD for anti-Siglec-7 treated mice slides and 83.69 ± 29.05 mean \pm SD for IgG1 treated mice slides $*p < 0.05$ (Figure 4C lower panel).

In a next step, we tested if the injection of Anti-Siglec-7 would be effective against established tumors. Following a different protocol, the first injection of Anti-Siglec-7 or of IgG1 ($8\mu\text{g}/\text{kg}$) was performed when HMC-1.1 engrafted SCID-beige mice displayed palpable tumors, i.e. day 20; and thereafter injections were performed every other day until the tumor size reached ~ 1.5 cm (Figure 4D). Remarkably, treatment with Anti-Siglec-7 significantly inhibited and sometimes even abolished the growth of the established HMC-1.1 tumors as evidenced a substantial reduction of tumor weight in Anti-Siglec-7 treated mice compared to that measured in IgG1 control -treated mice ($26. \pm 4$ mean \pm SD for anti-Siglec-7 treated mice and 173 ± 32 mean \pm SD for IgG1 treated mice (n=18 mice from 2 different pooled experiments $p^{***} < .0005$) (Figure 4E). Moreover, in this model a pronounced de-phosphorylation of the anti-apoptotic molecule Bcl-2 was found in tumor lysates obtained from the Anti-Siglec-7 as compared to the IgG1 treated mice (Figure 4F).

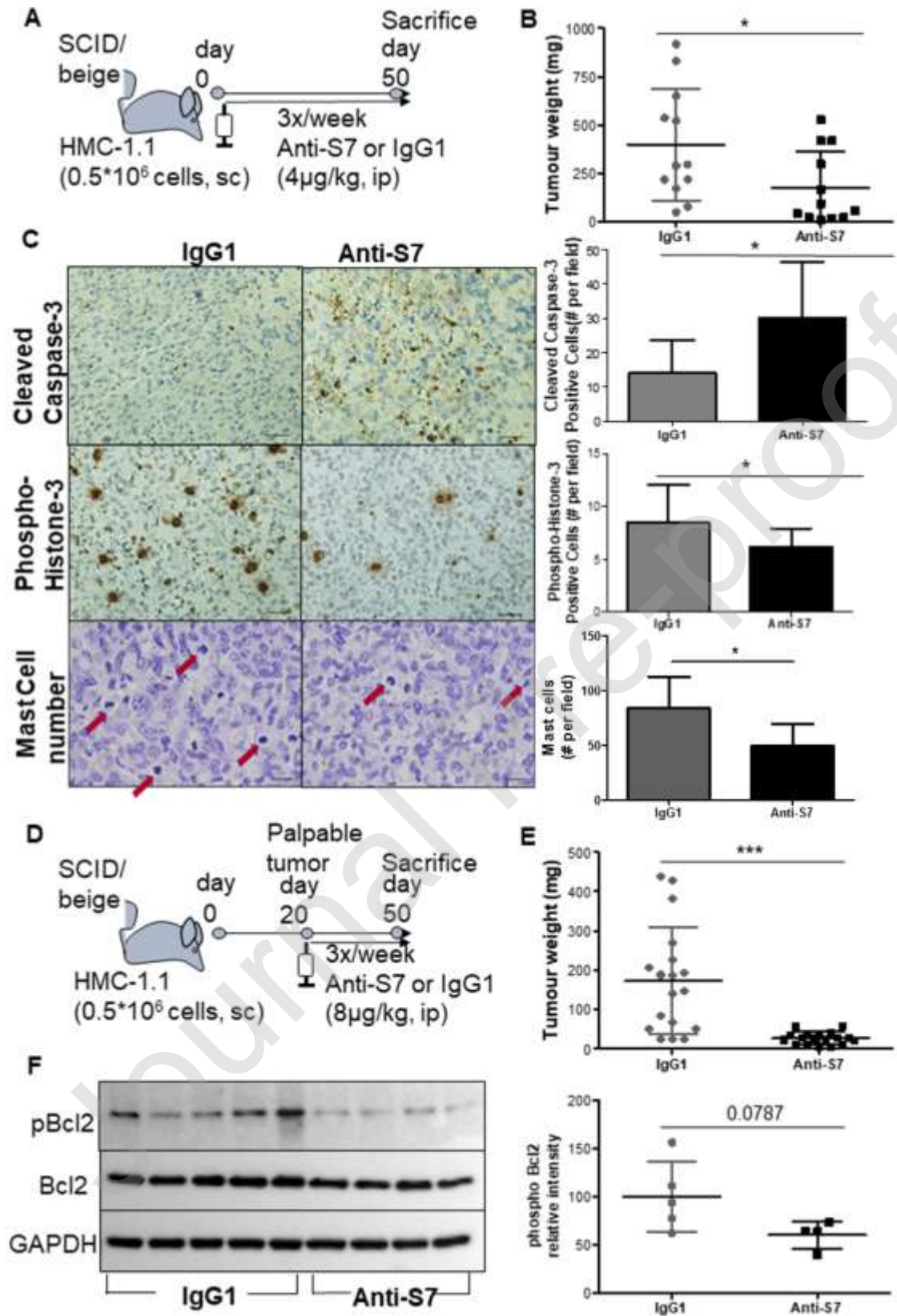


Figure 4- Anti-Siglec-7 inhibits the development of HMC-1.1 tumor growth in SCID/beige mice by apoptosis and by cell cycle arrest.

(A) Schematic representation of the treatment schedule of HMC-1.1 cells grafted mice. Anti-Siglec-7 injection started immediately after cell inoculation. HMC-1.1 cells ($0.5 \times 10^6 / 100 \mu\text{l}$) were injected subcutaneously (sc) into SCID-beige mice at day 0. Intraperitoneal injections (ip) of Anti-Siglec-7 or IgG1 (each $4 \mu\text{g}/\text{kg}$) were performed at 30 min, 24 h later and then every other day until tumors reached 1.5 cm and mice were euthanized. (B) Tumor weight (mg) of Anti-Siglec-7 or IgG1 treated mice as described in (A), Results represent the mean \pm SD of 2 independent experiments. (n=12 mice from 2 different pooled experiments) * $p < .05$ (C) Immunohistochemistry of tumor sections from mice treated with Anti-Siglec-7 or IgG1 stained with anti-cleaved Caspase-3 or anti-Phospho-Histone-3 or Toluidine Blue and densitometric quantification (positive cells, # per field). Left panels are photomicrographs of a representative experiment. Densitometry analyses (right panels) represent the mean \pm SD of 2 independent experiments for anti-cleaved Caspase-3, anti-Phospho-Histone 3 and for Toluidine blue staining. Red arrows indicate mast cells (MCs), Scale bars=100 μm . * $p < 0.05$ (D) HMC-1.1 cells ($0.5 \times 10^6 / 100 \mu\text{l}$) were injected sc into SCID-beige mice at day 0. Anti-Siglec-7 or IgG1 (each $8 \mu\text{g}/\text{kg}$) were injected ip at day 20 when the tumor became palpable, and then injected every other day until tumors reached 1.5 cm and mice were euthanized. (E) Tumor weight (mg) of Anti-Siglec-7 or IgG1 treated mice. Results represent the mean \pm SD of 2 independent experiments. (n=18 mice from 2 different pooled experiments) $p^{***} < .0005$ (F) Western Blot analysis for Bcl-2 phosphorylation of tumor tissue lysates from mice treated with Anti-Siglec-7 or IgG1. The blot shows 5 mice of each group.

3.5 Siglec-7 cytoplasmic domain contributes to Anti-Siglec-7 mediated anti-survival effects in vitro and in vivo.

The cytoplasmic domain of Siglec-7 contains two signaling motifs: a membrane-proximal ITIM, and a membrane-distal ITIM-like motif, both of which were shown to be involved in the recruitment of SHP-1 upon activation in NK cells(41). To investigate whether these motifs are essential for the Anti-Siglec-7 activity toward neoplastic target cells, we transduced the Siglec-7-negative human lymphoblastoid B cell line RPMI-8866 cells with empty vector containing GFP only (GFP⁺, used as control), full length Siglec-7 (CDS) and truncated Siglec-7 (Truncated) lacking the entire cytoplasmic tail. When the Siglec-7 expressing CDS cells were exposed to Anti-Siglec-7, a significant reduced cell viability was detected (MTT assay, 75 ± 8 mean \pm SD for anti-Siglec-7 treated CDS; 86 ± 7 mean \pm SD for anti-Siglec-7 treated Truncated cells at 72h; and 77 ± 10 mean \pm SD for anti-Siglec-7 treated CDS and 87 ± 4 mean \pm SD for anti-Siglec-7 treated Truncated cells at 96h Figure 5A) although, cells expressing truncated Siglec-7 were also inhibited even if at a lesser degree (Figure 5A). This indicates that *in vitro* the Siglec-7 tail takes part in its inhibitory effects, possibly together with other elements of the Siglec-7 receptor.

To further confirm the importance of the cytoplasmic domain of Siglec-7, we injected (sc) GFP⁺ or CDS or Truncated 8866 cells (0.5×10^6) into SCID-beige mice(40) followed by Anti-Siglec-7 (ip) as described above for HMC-1.1 (Figure 4A). We found, in line with our *in vitro* results, that treatment with Anti-Siglec-7 significantly reduced tumor growth in mice grafted with cells displaying full-length Siglec-7 (CDS). In fact, the tumor weight in these mice was significantly lower compared to the tumor weight in mice injected with cells expressing truncated Siglec-7 or with GFP⁺ control cells lacking Siglec-7 (148 ± 76 mg mean \pm SD for CDS tumor grafted mice;

379 ± 71 mg mean ± SD for truncated tumor grafted mice and 416 ± 89 mg mean ± SD for GFP⁺ tumor grafted mice; n=18 mice from 2 different pooled experiments *p< 0.05. Figure 5B).

Journal Pre-proof

Old figure 5:

NewFigure 5:

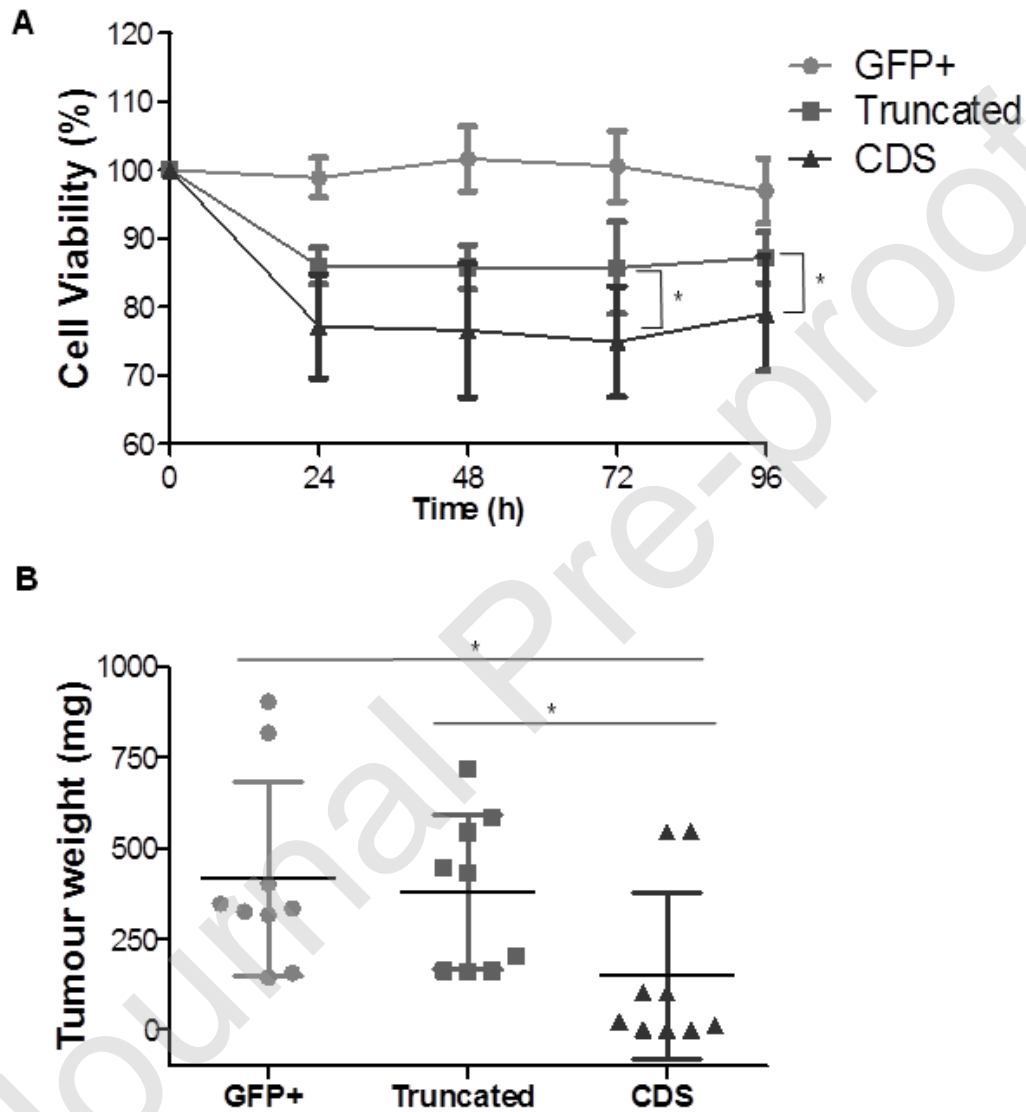


Figure 5- Siglec-7 cytoplasmic domain contributes to Anti-Siglec-7 mediated anti-survival effects *in vitro* and *in vivo*.

RPMI 8866 (8866) cells transfected either with GFP (GFP+, used as control), or with Siglec-7 extracellular domain without the cytoplasmic tail (Truncated) or with the intact Siglec-7 (CDS) were treated with Anti-Siglec-7 (10 µg/ml) or IgG1 (10 µg/ml) for different time points. **(A)** Cell viability (MTT assay). Data are shown as % of viable cells and expressed as mean ± SD of 5 independent experiments. *p <0.05. CDS vs. Truncated at 72 h and 96 h. **(B)** 8866 cells GFP+, Truncated or CDS (0.5×10^6 /100 µl) were injected subcutaneously (sc) into SCID-beige mice at day 0. Anti-Siglec-7 or IgG1 ip injections (4 µg/kg) were performed like described in 3A. Tumor weight (mg) of Anti-Siglec-7 treated GFP+ or Truncated or CDS tumors grafted mice. Results represent the mean ± SD of 2 independent experiments. (n=18 mice from 2 different pooled experiments) *p< 0.05.

4. Discussion

Treatment of advanced mastocytosis has substantially improved by the development of more selective and more potent tyrosine kinase inhibitors (17-19, 33) and ongoing efforts are now involving KIT D816V inhibitors (42). However, the disease is still incurable and most of the patients relapse or have resistant disease. Therefore, it is of crucial importance to identify novel therapeutic targets and to develop new improved anti-neoplastic therapies for these patients.

Previous reports have described some growth inhibition by activating either Siglec-2(43), Siglec-3(44), or to a much lesser degree Siglec-7(45) in AML cells and malignant B lymphocytes.

Here we investigated whether Siglec-7 can be harnessed to inhibit the growth of neoplastic MCs. We first examined Siglec-7 expression on primary MCs obtained from patients with mastocytosis and in several human MCL lines. As assessed by FC, MCs obtained from patients with ISM, advanced SM, including ASM, SM-AHN, and MCL, expressed Siglec-7 at comparable levels.

However, we observed variations in Siglec-7 expression levels between the SM patients that might be due to the fact that dead cell exclusion test was not applied. Furthermore, Siglec-7 was found to be expressed on MCs in control BM samples. These data suggest that Siglec-7 expression on MCs is neither dependent on oncogenic signaling networks nor on specific mutations in *KIT*. In addition, we were able to show that Siglec-7 is expressed on ROSA^{WT KIT} cells and ROSA^{KIT 816V} cells as we previously described for HMC-1.1 cells, HMC-1.2 harboring *KIT* D816V, and LAD2 cells (10).

Because of the limited availability of mastocytosis patients and the restricted MCs numbers that can be recovered from the patients' BM, we assessed Anti-Siglec-7 mediated effects in the MCL lines HMC-1.1(30) and LAD2(31). Anti-Siglec-7 reduced cell viability in a time-dependent fashion although no clear signs of apoptosis were displayed. This result was somehow expected. In fact, normal cells such as human cord blood derived MCs (10) and human peripheral blood eosinophils (13) incubated with Anti-Siglec-7, did not undergo cell death but rather inhibition of mediator release. It has also been shown that Anti-Siglec-7 on human monocytes mediates cytokine-production probably related to the presence of an activating form of Siglec-7 (46). Apoptotic mechanisms were, on the other hand, shown by incubation of platelets with the Siglec-7 natural ligand ganglioside GD2(47), suggesting that activation of Siglec-7 can sometimes also modulate survival-mediating processes, at least in platelets.

As other IR, Siglec-7 activation at least on NK cells, MCs and eosinophils has been demonstrated to lead to SHP-1 recruitment (13,38,48). Therefore we tested whether SHP-1 is phosphorylated following activation of Siglec-7 on HMC-1.1 and detected that it is significantly increased. SHP-1 is a known negative regulator of KIT (49-51). Siglec-7 activation of HMC-1.1 cells was found to induce KIT and some of its signal transduction molecules de-phosphorylation although not in a

significant fashion. These data show that the inhibitory cascade activated by Anti-Siglec-7 is mediated by SHP-1 and might impact directly or indirectly KIT downstream signaling pathways. Interestingly, we have previously demonstrated that in HMC-1.1 cells an anti-CD300a/anti-KIT bispecific antibody designed to activate the CD300a IR, caused SHIP-1 phosphorylation but not SHP-1, SYK and LAT de-phosphorylation but not KIT de-phosphorylation (52). The different results obtained by activating CD300a or Siglec-7 on HMC-1.1 might be due to the differences in the recruited phosphatase and adaptor molecules and demonstrate that SHP-1 is well-linked to KIT de-phosphorylation.

Using immuno-deficient SCID-beige mice that lack NK cells, grafted with HMC-1.1 cells, we found that Anti-Siglec-7 inhibits the growth of these tumors both when the mAb is administered immediately after the cell injection, and when the tumor is already established. These strong *in vivo* results, in comparison to the weaker *in vitro* ones, are nevertheless in line with them. Indeed, *in vivo* the inhibitory effects seem to be the result of anti-Siglec-7 induced KIT de-phosphorylation together with induction of apoptosis and cell cycle arrest, as shown by cleaved Caspase-3, de-phosphorylation of Bcl-2, and reduction of phospho-histone 3, that in concert result in reduced MCs numbers in the Anti-Siglec-7 treated tumors.

The strength of the *in vivo* data, in comparison to the *in vitro* ones, might be the result of a number of tumor microenvironment factors such as hypoxia, the expression of Siglec-7 ligand in the matrix, etc., rendering the tumor cells more sensitive to Anti-Siglec-7. Therefore, the lack of Anti-Siglec-7 effect on cell proliferation or cell death on primary patient-derived MCs (not shown) might be due to the “simplified” *in vitro* environment and /or to the specific patient and disease together with the specific drug treatment. Therefore, other tests with human primary mastocytosis cells are warranted.

To investigate whether the whole Siglec-7 receptor and consequent signal transduction are needed for the inhibitory effects, we transduced RPMI-8866 cells with empty vector containing GFP, full-length Siglec-7, and truncated Siglec-7 lacking the entire cytoplasmic tail. We observed *in vitro* that Anti-Siglec-7 strongly inhibited RPMI-8866 cells carrying full-length Siglec-7, but also moderately inhibited cells carrying only the extracellular portion of Siglec-7. Interestingly, clustering of Siglec-7 with a specific F(ab')₂ on the monocytic cell line U937 carrying Siglec-7 lacking the cytosolic ITIM domain, induced non-apoptotic cell death probably via ROS production by an unclear mechanism(53). Nevertheless, only the full length Siglec-7 cells had a significantly reduced tumor weight when treated with Anti-Siglec-7 *in vivo*.

Other members of the Siglec family, such as Sialoadhesin, Siglec-H or Siglec-14 have also been reported to function even when lacking the tyrosine-based signaling motif (7). Moreover, some ITIM bearing receptors have been described to act sometimes as positive regulators of cell functions and vice versa (54) complicating the whole scenario.

In conclusion, we have shown that primary neoplastic MCs from BM of mastocytosis patients, as human MC lines, express Siglec-7. Moreover, we demonstrated that activation of Siglec-7 inhibits the *in vitro* growth and viability of human MC lines and their *in vivo* growth in immune compromised mice. Finally, our data suggest that Siglec-7 mediates growth inhibition in transformed MCs by activating phosphorylation of SHP-1 and de-phosphorylation of KIT and of other signal transduction molecules. We therefore hypothesize that Anti-Siglec-7 mAb application may be a new promising approach to inhibit the growth of neoplastic MCs in patients with advanced mastocytosis.

Funding: This work was partially funded by grants from Aimwell Charitable Trust (UK), the Adolph and Klara Brettler Center of the Hebrew University's School of Pharmacy and from the Israel Science Foundation (ISF) to F.L-S.; from SAF2015-68124-R, issued by MINECO-FEDER (Spain-UE); and by *Instituto de Salud Carlos III* (ISCIII) co-founded by *Fondo Europeo de Desarrollo Regional* (FEDER) for the Thematic Networks and Co-operative Research Centres(ARADyAL, RD16/0006/0007) to MM.; from the Austrian Science Fund (FWF, project F4704-B20) to P.V.

Author contributions:

N.L: performed the experiments, analyzed the data and wrote the manuscript ; I.Z, D.S., E.S-C,D.S.: performed selected experiments, analyzed the relevant data; S.F. helped with the *in vivo* experiments; M.A. provided ROSA cells; K.H.,E.P., O.M., M.M. :conceptualization of selected experiments ;P.V: conceptualization, provided patient cells, supervised experiments with primary mast cells and cell lines, and correction and edition of manuscript draft; F.L-S.: conceptualization and supervision of the whole study, corrections and edition of manuscript drafts; and all authors reviewed the final manuscript.

Conflict-of-interest disclosure

The authors declare no competing interests.

Ethics approval

The animal studies were reviewed and approved by the Ethics Committee for Animal Studies at the Hebrew University. The human data was approved by the ethics committee of the Medical University of Vienna. All patients gave written informed consent before BM puncture.

Consent for publication

All authors agreed on the manuscript.

Availability of data and materials

The datasets used and/or analyzed during this study are available from the corresponding author on request.

Acknowledgments:

The authors would like to thank Flavio Forte; Dr Saar Mizrahi; Dr Elad Horwitz for technical advices; and Prof. Renato Bernardini; Prof. Giuseppina Cantarella; and Prof David Mankuta for helpful discussions.

References:

1. Billadeau DD, Leibson PJ. ITAMs versus ITIMs: striking a balance during cell regulation. *J Clin Invest.* 2002; 109(2):161-8.
2. Pani G, Fischer KD, Mlinaric-Rascan I, Siminovitch KA. Signaling capacity of the T cell antigen receptor is negatively regulated by the PTP1C tyrosine phosphatase. *J Exp Med.* 1996; 184(3):839-52.
3. Zhang L, Oh SY, Wu X, Oh MH, Wu F, Schroeder JT, Takemoto CM, Zheng T, Zhu Z. SHP-1 deficient mast cells are hyperresponsive to stimulation and critical in initiating allergic inflammation in the lung. *J Immunol.* 2010; 184(3): 1180-90.
4. Thangaraju M, Sharma K, Leber B, Andrews DW, Shen SH, Srikant CB. Regulation of acidification and apoptosis by SHP-1 and Bcl-2. *J Biol Chem.* 1999; 274(41): 29549-57.
5. Chuang YF, Huang SW, Hsu YF, Yu MC, Ou G, Huang WJ, Hsu MJ. WMJ-8-B, a novel hydroxamate derivative, induces MDA-MB-231 breast cancer cell death via the SHP-1-STAT3-survivin cascade. *Br J Pharmacol.* 2017;174(17):2941-2961.
6. Chiu YH, Lee YY, Huang KC, Liu CC, Lin CS. Dovitinib Triggers Apoptosis and Autophagic Cell Death by Targeting SHP-1/p-STAT3 Signaling in Human Breast Cancers. *J Oncol.* 2019; doi: 10.1155/2019/2024648.
7. Crocker PR, Paulson JC, Varki A. Siglecs and their roles in the immune system. *Nat Rev Immunol.* 2007; 7(4):255-66.
8. Nicoll G, Ni J, Liu D, Klenerman P, Munday J, Dubock S, Mattei MG, Crocker PR. Identification and characterization of a novel siglec, siglec-7, expressed by human natural killer cells and monocytes. *J Biol Chem.* 1999; 274(48): 34089-95.

9. Fraschilla I, Pillai S. Viewing Siglecs through the lens of tumor immunology. *Immunol Rev.* 2017; 276(1): 178-91.
10. Mizrahi S, Gibbs BF, Karra L, Ben-Zimra M, Levi-Schaffer F. Siglec-7 is an inhibitory receptor on human mast cells and basophils. *J Allergy Clin Immunol.* 2014; 134(1): 230-3.
11. Munitz A, Bachelet I, Eliashar R, Moretta A, Moretta L, Levi-Schaffer F. The inhibitory receptor IRp60 (CD300a) suppresses the effects of IL-5, GM-CSF, and eotaxin on human peripheral blood eosinophils. *Blood.* 2006; 107(5):1996-2003.
12. Kawasaki Y, Ito A, Withers DA, Taima T, Kakoi N, Saito S, Arai Y. Ganglioside DSGb5, preferred ligand for Siglec-7, inhibits NK cell cytotoxicity against renal cell carcinoma cells. *Glycobiology.* 2010; 20(11):1373-9.
13. Legrand F, Landolina N, Zaffran I, Emeh RO, Chen E, Klion AD, Levi-Schaffer F. Siglec-7 on peripheral blood eosinophils: surface expression and function. *Allergy.* 2019; 74(7): 1257-1265.
14. Vitale C, Romagnani C, Puccetti A, Olive D, Costello R, Chiossone L, Pitto A, Bacigalupo A, Moretta L, Mingari MC. Surface expression and function of p75/AIRM-1 or CD33 in acute myeloid leukemias: engagement of CD33 induces apoptosis of leukemic cells. *Proc Natl Acad Sci U S A.* 2001; 98(10): 5764-9.
15. Vitale C, Romagnani C, Falco M, Ponte M, Vitale M, Moretta A, Bacigalupo A, Moretta L, Mingari MC. Engagement of p75/AIRM1 or CD33 inhibits the proliferation of normal or leukemic myeloid cells. *Proc Natl Acad Sci U S A.* 1999; 96(26): 15091-6.
16. Valent P, Horny HP, Escribano L, Longley BJ, Li CY, Schwartz LB, Marone G, Nuñez R, Akin C, Sotlar K, et al. Diagnostic criteria and classification of mastocytosis: a consensus proposal. *Leuk Res.* 2001; 25(7): 603-25.

17. Valent P, Akin C, Metcalfe DD. Mastocytosis: 2016 updated WHO classification and novel emerging treatment concepts. *Blood*. 2017; 129(11):1420-7.
18. Metcalfe DD, Mekori YA. Pathogenesis and Pathology of Mastocytosis. *Annu Rev Pathol*. 2017;12:487-514.
19. Valent P, Akin C, Hartmann K, Nilsson G, Reiter A, Hermine O, Sotlar K, Sperr WR, Escribano L, George TI, et al. Advances in the Classification and Treatment of Mastocytosis: Current Status and Outlook toward the Future. *Cancer Res*. 2017; 77(6): 1261-70.
20. Akin C. Mast cell activation syndromes. *J Allergy Clin Immunol*. 2017; 140(2): 349-55.
21. Nagata H, Worobec AS, Oh CK, Chowdhury BA, Tannenbaum S, Suzuki Y, Metcalfe DD. Identification of a point mutation in the catalytic domain of the protooncogene c-kit in peripheral blood mononuclear cells of patients who have mastocytosis with an associated hematologic disorder. *Proc Natl Acad Sci U S A*. 1995; 92(23):10560-4.
22. Falchi L, Verstovsek S. Kit Mutations: New Insights and Diagnostic Value. *Immunol Allergy Clin North Am*. 2018; 38(3): 411-28.
23. Arock M, Sotlar K, Akin C, Broesby-Olsen S, Hoermann G, Escribano L, Kristensen TK, Kluin-Nelemans HC, Hermine O, Dubreuil P, et al. KIT mutation analysis in mast cell neoplasms: recommendations of the European Competence Network on Mastocytosis. *Leukemia*. 2015; 29(6): 1223-32.
24. Furitsu T, Tsujimura T, Tono T, Ikeda H, Kitayama H, Koshimizu U, Sugahara H, Butterfield JH, Ashman LK, Kanayama Y, et al. Identification of mutations in the coding sequence of the proto-oncogene c-kit in a human mast cell leukemia cell line causing ligand-independent activation of c-kit product. *J Clin Invest*. 1993; 92(4):1736-44.

25. Piao X, Bernstein A. A point mutation in the catalytic domain of c-kit induces growth factor independence, tumorigenicity, and differentiation of mast cells. *Blood*. 1996; 87(8): 3117-23.
26. Longley BJ, Jr., Metcalfe DD, Tharp M, Wang X, Tyrrell L, Lu SZ, Heitjan D, Ma Y. Activating and dominant inactivating c-KIT catalytic domain mutations in distinct clinical forms of human mastocytosis. *Proc Natl Acad Sci U S A*. 1999; 96(4): 1609-14.
27. Baumgartner C, Cerny-Reiterer S, Sonneck K, Mayerhofer M, Gleixner KV, Fritz R, Kerenyi M, Boudot C, Gouilleux F, Kornfeld JW, et al. Expression of activated STAT5 in neoplastic mast cells in systemic mastocytosis: subcellular distribution and role of the transforming oncoprotein KIT D816V. *Am J Pathol*. 2009; 175(6): 2416-29.
28. Harir N, Boudot C, Friedbichler K, Sonneck K, Kondo R, Martin-Lannere S, Kenner L, Kerenyi M, Yahiaoui S, Gouilleux-Gruart V, et al. Oncogenic Kit controls neoplastic mast cell growth through a Stat5/PI3-kinase signaling cascade. *Blood*. 2008; 112(6): 2463-73.
29. Gabillot-Carre M, Lepelletier Y, Humbert M, de Sepuvelde P, Hamouda NB, Zappulla JP, Liblau R, Ribadeau-Dumas A, Machavoine F, Letard S, et al. Rapamycin inhibits growth and survival of D816V-mutated c-kit mast cells. *Blood*. 2006; 108(3): 1065-72.
30. Sundstrom M, Vliagoftis H, Karlberg P, Butterfield JH, Nilsson K, Metcalfe DD, Nilsson G. Functional and phenotypic studies of two variants of a human mast cell line with a distinct set of mutations in the c-kit proto-oncogene. *Immunology*. 2003; 108(1): 89-97.
31. Kirshenbaum AS, Akin C, Wu Y, Rottem M, Goff JP, Beaven MA, Rao VK, Metcalfe DD. Characterization of novel stem cell factor responsive human mast cell lines LAD 1 and 2 established from a patient with mast cell sarcoma/leukemia; activation following aggregation of FcepsilonRI or FcgammaRI. *Leuk Res*. 2003; 27(8):677-82.

32. Saleh R, Wedeh G, Herrmann H, Bibi S, Cerny-Reiterer S, Sadovnik I, Blatt K, Hadzijusufovic E, Jeanningros S, Blanc C, et al. A new human mast cell line expressing a functional IgE receptor converts to tumorigenic growth by KIT D816V transfection. *Blood*. 2014; 124(1): 111-20.
33. Valent P, Akin C, Hartmann K, George TI, Sotlar K, Peter B, Gleixner KV, Blatt K, Sperr WR, Manley PW, et al. Midostaurin: a magic bullet that blocks mast cell expansion and activation. *Ann Oncol*. 2017; 28(10): 2367-76.
34. Gotlib J, Kluijn-Nelemans HC, George TI, Akin C, Sotlar K, Hermine O, Awan FT, Hexner E, Mauro MJ, Sternberg DW, et al. Efficacy and Safety of Midostaurin in Advanced Systemic Mastocytosis. *N Engl J Med*. 2016; 374(26): 2530-41.
35. Gotlib J, Gerds AT, Bose P, Castells MC, Deininger MW, Gojo I, Gundabolu K, Hobbs G, Jamieson C, McMahon B, et al. Systemic Mastocytosis, Version 2.2019, NCCN Clinical Practice Guidelines in Oncology. *J Natl Compr Canc Netw*. 2018;16 (12): 1500-37.
36. Bibi S, Arock M. Tyrosine Kinase Inhibition in Mastocytosis: KIT and Beyond KIT. *Immunol Allergy Clin North Am*. 2018; 38(3): 527-43.
37. Butterfield JH, Weiler D, Dewald G, Gleich GJ. Establishment of an immature mast cell line from a patient with mast cell leukemia. *Leuk Res*. 1988; 12(4): 345-55.
38. Falco M, Biassoni R, Bottino C, Vitale M, Sivori S, Augugliaro R, Moretta L, Moretta A. Identification and molecular cloning of p75/AIRM1, a novel member of the sialoadhesin family that functions as an inhibitory receptor in human natural killer cells. *J Exp Med*. 1999; 190(6): 793-802.

39. Kozlowski M, Larose L, Lee F, Le DM, Rottapel R, Siminovitch KA. SHP-1 binds and negatively modulates the c-Kit receptor by interaction with tyrosine 569 in the c-Kit juxtamembrane domain. *Mol Cell Biol*. 1998;18 (4) :2089-99.
40. Morton CL, Houghton PJ. Establishment of human tumor xenografts in immunodeficient mice. *Nat Protoc*. 2007;2(2): 247-50.
41. Yamaji T, Mitsuki M, Teranishi T, Hashimoto Y. Characterization of inhibitory signaling motifs of the natural killer cell receptor Siglec-7: attenuated recruitment of phosphatases by the receptor is attributed to two amino acids in the motifs. *Glycobiology*. 2005; 15(7):667-76.
42. Shomali W, Gotlib J. The new tool "KIT" in advanced systemic mastocytosis. *Hematology Am Soc Hematol Educ Program*. 2018(1):127-136.
43. Haas KM, Sen S, Sanford IG, Miller AS, Poe JC, Tedder TF. CD22 ligand binding regulates normal and malignant B lymphocyte survival in vivo. *J Immunol*. 2006; 177(5):3063-73.
44. Laszlo GS, Harrington KH, Gudgeon CJ, Beddoe ME, Fitzgibbon MP, Ries RE, Lamba JK, McIntosh MW, Meshinchi S, Walter RB. Expression and functional characterization of CD33 transcript variants in human acute myeloid leukemia. *Oncotarget*. 2016; 7(28): 43281-43294.
45. Mingari MC, Vitale C, Romagnani C, Falco M, Moretta L. p75/AIRM1 and CD33, two sialoadhesin receptors that regulate the proliferation or the survival of normal and leukemic myeloid cells. *Immunol Rev*. 2001;181:260-8.
46. Varchetta S, Brunetta E, Roberto A, Mikulak J, Hudspeth KL, Mondelli MU, Mavilio D. Engagement of Siglec-7 receptor induces a pro-inflammatory response selectively in monocytes. *PLoS One*. 2012;7(9):e45821

47. Nguyen KA, Hamzeh-Cognasse H, Palle S, Anselme-Bertrand I, Arthaud CA, Chavarin P, Pozzetto B, Garraud O, Cognasse F. Role of Siglec-7 in apoptosis in human platelets. *PloS One*. 2014; 9(9):e106239.
48. Bachelet I, Munitz A, Moretta A, Moretta L, Levi-Schaffer F. The inhibitory receptor IRp60 (CD300a) is expressed and functional on human mast cells. *J Immunol*. 2005; 175(12): 7989-95.
49. Qu X, Zhang S, Wang S, Wang Y, Li W, Huang Y, Zhao H, Wu X, An C, Guo X, et al. TET2 deficiency leads to stem cell factor dependent clonal expansion of dysfunctional erythroid progenitors. *Blood*. 2018; 132(22): 2406-2417.
50. Raghav PK, Singh AK, Gangenahalli G. Stem cell factor and NSC87877 combine to enhance c-Kit mediated proliferation of human megakaryoblastic cells. *PloS One*. 2018; 13(11): e0206364.
51. Raghav PK, Singh AK, Gangenahalli G. A change in structural integrity of c-Kit mutant D816V causes constitutive signaling. *Mutat Res*. 2018;808:28-38.
52. Bachelet I, Munitz A, Berent-Maoz B, Mankuta D, Levi-Schaffer F. Suppression of normal and malignant kit signaling by a bispecific antibody linking kit with CD300a. *J Immunol*. 2008; 180(9): 6064-9.
53. Mitsuki M, Nara K, Yamaji T, Enomoto A, Kanno M, Yamaguchi Y, Yamada A, Waguri S, Hashimoto Y. Siglec-7 mediates nonapoptotic cell death independently of its immunoreceptor tyrosine-based inhibitory motifs in monocytic cell line U937. *Glycobiology*. 2010; 20(3):395-402.
54. Barrow AD, Trowsdale J. You say ITAM and I say ITIM, let's call the whole thing off: the ambiguity of immunoreceptor signalling. *Eur J Immunol*. 2006;36(7):1646-53.

55. Ruifrok AC, Johnston DA. Quantification of histochemical staining by color deconvolution. *Anal Quant Cytol Histol.* 2001; 23:291-9.

Journal Pre-proof